Spatial Transcriptomic Analysis Identifies Epithelium-Macrophage Crosstalk in Endometriotic Lesions

Gregory W. Burns[1], Zhen Fu[2], Erin L. Vegter[1], Zachary B. Madaj[2], Erin Greaves[3], Idhaliz Flores[4], and Asgerally T. Fazleabas[1]*

[1]Department of Obstetrics, Gynecology and Reproductive Biology, Michigan State University, Grand Rapids, MI, USA

[2]Bioinformatics and Biostatistics, Van Andel Institute, Grand Rapids, MI, USA

[3]Division of Biomedical Sciences, University of Warwick, Coventry, UK

[4]Deptartment of Basic Sciences, Ponce Research Institute, Ponce Health Sciences University, Ponce, PR, USA

*Corresponding author
Email: fazleaba@msu.edu
Address: 400 Monroe Ave NW, GRRC 3020, Grand Rapids, MI 49503 USA
Telephone: +1 616-234-0981

Abstract

The mechanisms underlying the pathophysiology of endometriosis, characterized by the presence of endometrium-like tissue outside the uterus, remain poorly understood. This study aimed to identify cell type-specific gene expression changes in superficial peritoneal endometriotic lesions and elucidate the crosstalk among the stroma, epithelium, and macrophages compared to patient-matched eutopic endometrium. Surprisingly, comparison between lesions and eutopic endometrium revealed transcriptional similarities, indicating minimal alterations in the sub-epithelial stroma and epithelium of lesions. Spatial transcriptomics highlighted increased signaling between the lesion epithelium and macrophages, emphasizing the role of the epithelium in driving lesion inflammation. We propose that the superficial endometriotic lesion epithelium orchestrates inflammatory signaling and promotes a pro-repair phenotype in macrophages, providing a new role for Complement 3 in lesion pathobiology. This study underscores the significance of considering spatial context and cellular interactions in uncovering mechanisms governing disease in endometriotic lesions.

Introduction

Endometriosis affects around 10% of reproductive age women and is defined by the presence of endometrium-like tissue growing outside of the uterus [1-3]. The disease is clinically associated with life-altering pain and infertility and up to 50% of infertile women are diagnosed with endometriosis [4, 5]. Endometriotic lesions are estrogen-dependent and the only effective non-surgical treatment is suppression of ovarian function to limit estrogen production. Endometriotic lesions in the peritoneal cavity are classified by location with lesions present on the visceral or parietal peritoneum termed peritoneal lesions and those on the ovary termed endometriomas. Peritoneal lesions are further separated into superficial or deep infiltrating according to the invasion depth of underlying tissue with deep infiltrating lesions invading more than 5 mm [6, 7]. Superficial peritoneal endometriotic lesions likely develop from endometrial tissue fragments that are refluxed into the peritoneal cavity during menstruation [8, 9]. This hypothesis is supported by the baboon model of endometriosis in which menstrual tissue inoculated into the peritoneal cavity results in endometriotic lesions and disease that persists for at least 15 months [10-12]. Endometriosis can also be induced in mice with tissue collected from an artificial menstruation cycle [13, 14]. Superficial peritoneal lesions generally consist of endometrium-like epithelium and stroma, fibroblasts that express smooth muscle actin (ACTA2), and immune cells [15]. The presence of ACTA2+ fibroblasts is positively correlated with fibrotic lesions where the presence of epithelium is less common, in contrast to lesions of endometrium-like stroma and epithelium [16, 17]. During lesion development, activation of pro-inflammatory immune populations, specifically macrophages, provides a hospitable inflammatory environment to protect the ectopic endometrial tissue [18]. Previous bulk and single cell-RNA sequencing analyses identified thousands of differentially expressed genes (DEG) in endometriotic lesions, including inflammation- and immune-related genes [19-23]. Our aim was to determine the genes and pathways altered in the glandular epithelium, stroma, and macrophages within endometriotic

54 lesions compared to matched endometrium with spatial transcriptomics. Spatial transcriptomics
55 has emerged as a powerful tool for understanding the spatial context of gene expression within
56 tissues, strengthened by the addition of canonical cell type immunostaining. Two of the most
57 prominent platforms for spatial transcriptomics, nanoString GeoMx and 10X Visium, offer distinct
58 advantages and limitations depending on experimental design. In this study, we chose the GeoMx
59 platform based on the ability to provide cell type specific data from formalin fixed paraffin
60 embedded (FFPE) tissues with high specificity based on antibody-based fluorescent
61 segmentation [24-26]. We hypothesized that gene expression changes in superficial peritoneal
62 endometriotic lesions would manifest in a cell type-specific manner, with disruption of the crosstalk
63 among the stroma, epithelium, and macrophages being evident compared to patient-matched
64 eutopic endometrium.

65 Results

66 Spatial Transcriptomics of Human Superficial Peritoneal Lesions

67 We sought to determine the contributions of epithelium, stroma, and myeloid cell
68 compartments of endometriotic lesions to altered genes and pathways in endometriotic lesions
69 by spatial transcriptomic analyses. Superficial peritoneal lesions and eutopic uterine tissue were
70 collected from women in the secretory phase of the menstrual cycle. Matched lesion and eutopic
71 tissues from five women (n = 10) were selected based on the histological presence of endometrial
72 gland-like structures in lesions confirmed by trichrome staining (Figure 1). The average age of the
73 patients was 42 (Table 1, SD = 6.1). Tissues were stained for pan-cytokeratin, smooth muscle
74 actin, and CD68 to identify epithelium (pan-cytokeratin+), stroma (ACTA2) and myeloid-lineage
75 cells (CD68+, monocytes and macrophages). Myeloid cells were present in both eutopic
76 endometrium and endometriotic lesions within stromal and epithelial compartments (Figure 1).
77 ACTA2+ cells were present in the vasculature and stroma, although not in the immediate sub-

epithelial stroma. Duplicate regions of interest were selected for each tissue and segmented based on fluorescence intensity for macrophages, epithelium, and stroma, resulting in 60 segments.

Based on the limit of quantification, 10 segments were removed with a gene detection rate of lower than 10% (Figure 2A). Read counts were normalized for the remaining 50 segments using the quartile 3 (Q3) method. Separation between the geometric mean of the negative control probes and Q3 of gene read counts was confirmed at the segment and distribution levels to ensure compatibility with Q3 normalization (Figure 2B). Next, genes detected in less than 10% of segments were removed leaving 7,945 genes (Figure 2C). Overall gene expression across segments was visualized with a Uniform Manifold Approximation and Projection (UMAP) plot, which resulted in two major clusters (Figure 2D). Epithelial segments were contained in one cluster and the second cluster included both stroma and macrophage segments. Notably, segments from the same patient were found in close proximity within each cluster.

Epithelium and Stroma Marker Genes Are Similar in Lesions and Endometrium

We compared the epithelium and stroma segments by tissue type to confirm cell type separation and identify differences in the cell identity in the lesion tissue. The eutopic endometrial epithelium was compared to matching stroma and 1,372 DEG corresponding to cell type were found (Figure 3A). Similarly, there were 1,313 DEG in lesion epithelium versus stroma (Figure 3B) and 14 of the top 20 genes were in common. Gene expression patterns were similar in the endometrium and lesion tissues with a correlation coefficient of 0.81 ($p < 2.2 \times 10^{-16}$, Figure 3C). Stromal and epithelial biological process terms were distinct and consistent with cell type (Figure 4D). Vascularization, extracellular matrix, and cell adhesion terms were enriched in the stroma while epithelial cell differentiation and cell-cell junction terms were enriched in the epithelium. Terms were very similar in the stroma with 9 of 10 terms common between the eutopic endometrium and lesions. However, five terms were unique to the lesion epithelium, related to

103 cell-cell adhesion and cell projections or cilia, and two terms to the eutopic endometrial epithelium,
104 cellular transition metal ion homeostasis and circulatory system process.

105 Endometriotic Stroma is Minimally Altered

106 The sub-epithelial stroma from lesions was compared to matched eutopic endometrium to
107 determine transcriptome alterations in endometriotic lesions. Separation of eutopic stroma from
108 the lesions was strongest on PC3, accounting for 12.37% of variation in the dataset (Figure 4A).
109 Two downregulated genes were identified in lesions (Figure 4B), *DHRS1*,
110 dehydrogenase/reductase 1, and *SCGB2A1*, secretoglobin family 2A member 1, both related to
111 steroid metabolism. Six hallmark gene sets [27] were significant in a GSEA, four increased and
112 two decreased (Figure 4C). The increased gene sets were inflammation-related, TNFα signaling
113 via NF-κB, interferon gamma response, interferon alpha response, and inflammatory response,
114 and the decreased gene sets were MYC targets V1 and epithelial mesenchymal transition.

115 Immune Response is Increased in the Endometriotic Lesion Epithelium

116 The endometriotic epithelium was compared to the matched eutopic glandular epithelium
117 and was most separated from the eutopic endometrial epithelium on PC3, representing 9.45% of
118 variation in gene expression (Figure 5A). Differential expression analysis found 76 DEG with 33
119 increased in the lesion epithelium and 43 decreased (Figure 5B). Notably, multiple immune-
120 related genes were increased including, *C3*, or complement 3, *CD74*, *CLU*, or clusterin, and major
121 histocompatibility complex class II members *HLA-DRB1* and *HLA-DPB1*. There were 10
122 significant hallmark gene sets from a GSEA with four terms increased and six decreased (Figure
123 5C). Among the increased gene sets were interferon gamma response and allograft rejection,
124 which matched the increase in immune-related genes in the volcano plot. Genes decreased in
125 response to damage by UV radiation, a source of tissue damage and inflammation, were
126 decreased in lesions. Compared to the eutopic endometrium, glycolysis, angiogenesis, androgen
127 response, and epithelial mesenchymal transition gene sets were decreased in the lesion

128 epithelium. Genes increased in the lesion epithelium were enriched for 33 gene ontology (GO)
129 biological process terms and nine of the top 10 were related to immune response (Figure 5D). In
130 fact, nine of the 33 upregulated genes were associated with positive regulation of immune
131 response: *CD74*, *HLA-DRB1*, *CLU*, *C3*, *HLA-DPB1*, *RPS19*, *HLA-DQB1*, *CFB*, and *VTCN1*.

132 Neither Stroma nor Epithelium Clustered by Tissue

133 Hierarchical clustering dendrograms were plotted for the stromal and epithelial segments
134 (Figures 6A-B) as an unsupervised measure of segment similarity. Neither cell type clustered by
135 eutopic or lesion origin. Segments from two patients were clustered in the stroma and epithelium,
136 that is lesion segments were more like eutopic tissue from the same patient than another lesion.
137 Principal component analyses of the stroma and epithelium (Figures 6C-D) segments revealed
138 that PC1 was driven by patient ID, representing 23.28% and 16.68% of variation in gene
139 expression, respectively.

140 Macrophages are Altered in Peritoneal Lesions

141 Lesion macrophages were most separated from eutopic endometrium macrophages on
142 PC3, representing 8.87% of variation in gene expression (Figure 7A). Differential expression
143 analysis found 148 DEG with 35 increased and 113 decreased in the lesion macrophages (Figure
144 7B). Nine hallmark gene sets were significantly enriched from a GSEA with seven terms increased
145 and two decreased (Figure 7C). The seven increased terms were associated with inflammation
146 and included TNFα signaling via NF-κB, inflammatory response, allograft rejection, and IL2
147 STAT5 signaling. Gene sets that were decreased were myogenesis and epithelial mesenchymal
148 transition.

149 To provide context for our findings, we sought to compare our results with bulk sequencing
150 data from human peritoneal lesions [21]. Human peritoneal lesions were separated from eutopic
151 endometrium on principal component (PC) one (39.43% of variation) and 3,656 differentially
152 expressed genes (DEG) were identified in an analysis of bulk RNA-sequencing data

153 (Supplemental Figures 1A-C). Gene set enrichment analysis (GSEA) [28] found TNFα signaling
154 via NF-κB, myogenesis, immune response, and adipogenesis hallmark genes [27] increased,
155 while estrogen response, glycolysis, and multiple cell cycle gene sets were decreased in
156 endometriotic lesions (Supplemental Figure 1D).

157 Ligand-Receptor Analysis Identified Epithelium-Macrophage Signaling Axis in 158 Lesions

159 CellChat [29] ligand-receptor analysis was performed to determine the cell-cell
160 communication landscape in endometriotic lesions and eutopic endometrium. Based on 976
161 significant ligand-receptor interactions, 29 signaling pathways were identified in total. Twenty-six
162 pathways were present in lesions, 24 in the endometrium, and 21 pathways were common to
163 both. Three pathways were unique to the endometrium, CXCL, SPP1, and TGF-β, and five unique
164 to lesions, CD45, CD46, ITGB2, PTPRM, and SEMA3. A heatmap of signaling pathways
165 consisting of all possible connections, inter- and intra-tissue, ranked by signaling strength (Figure
166 8A) found collagen signaling to be the strongest followed by MHC-II, laminin, macrophage
167 migration inhibitory factor (MIF) and complement. The three top interacting cell types were lesion
168 stroma, endometrium stroma, and lesion macrophages. Visualization of the cell-cell
169 communication networks in the endometrium and lesions by weight in circle plots showed strong
170 connections from the stroma compartment to the epithelium in both tissue types (Figure 8B).
171 Based on combined network weights, confined to tissue type, the top senders were endometrial
172 (0.172) and lesion stroma (0.170), and the top receivers were lesion macrophages (0.184) and
173 epithelium (0.104). Particularly striking was a 3.70-fold increase in epithelium-to-macrophage
174 signaling in lesions compared to eutopic endometrium. Interaction strength heatmaps (Figure 8C),
175 confirmed the strong connection from the endometrial stroma received by the epithelium. In
176 lesions, the strongest interaction was macrophage-macrophage signaling followed by epithelium-

177 macrophage, surpassing stroma to epithelium signaling. These results point to a strengthened
178 epithelium-macrophage signaling axis in endometriotic lesions.

179 Given that multiple inflammatory pathways were increased in lesions, including MHC-II
180 and complement, and since increased signaling was noted between the lesion epithelium and
181 macrophages, we sought to determine the source of inflammation-related ligands in lesions. A
182 ligand-receptor bubble plot (Figure 9A) demonstrated that complement and MHC-II ligands were
183 originating in the lesion epithelium and likely binding to receptors on macrophages. Within the
184 stroma, MIF was the only visualized inflammatory pathway with likely communication probability
185 indicating that inflammatory signals originated largely in the lesion epithelium. Indeed, a chord
186 diagram of complement signaling (Figure 9B) highlighted the increased complement signaling
187 present in lesions compared to the endometrium and the lesion epithelium as the source.

188 Discussion

189 Endometriosis is a complex reproductive disorder marked by the presence of
190 endometrium-like tissue outside the uterus. Focusing on superficial peritoneal lesions, and
191 excluding deep infiltrating or ovarian endometrioma disease, we hypothesized that endometrium-
192 like tissue in these lesions would display an altered molecular phenotype influenced by the
193 peritoneal microenvironment. To explore this hypothesis, we utilized spatial transcriptomic,
194 receptor-ligand, and bulk RNA-sequencing analyses of endometriotic lesions compared to eutopic
195 endometrium.

196 Bulk RNA-sequencing unveiled thousands of differentially expressed genes (DEGs) and
197 numerous altered inflammatory pathways in lesions compared to the eutopic endometrium,
198 highlighting the inflammatory nature of these lesions and the presence of fibrotic tissue. This
199 observation supported the notion that endometrium-like tissue within the peritoneum would differ
200 significantly from its uterine counterpart. Inflammatory cytokines are increased in the peritoneal
201 fluid of women with endometriosis [30], likely influencing gene expression. Indeed, miRNAs,

202 Notch signaling, aromatase enzymes, prostaglandins, and progestin responsiveness are altered
203 in lesions compared to matched endometrial tissues [31-42].

204 Contrary to our initial expectations, spatial analysis revealed transcriptomic similarities
205 between the three major cell types found in endometrium-like regions of lesions and patient-
206 matched eutopic endometrium, with macrophages displaying the most substantial transcriptional
207 difference. This lack of transcriptional divergence in the epithelium and stroma supports the idea
208 that superficial peritoneal endometriotic lesions are derived from the endometrium following
209 retrograde menstruation [8, 9]. Further, patient rather than tissue type, that is lesion or
210 endometrium, was the primary determinant of gene expression based on principal component
211 and UMAP plots. The differences observed in macrophage gene expression are likely due to the
212 presence of peritoneal and monocyte-derived macrophages in lesions, compared to tissue
213 resident macrophages in the eutopic endometrium [43-45].

214 The discrepancy between bulk RNA-seq and spatial analyses points to the inherent
215 differences in methodologies. While bulk RNA-seq provides a comprehensive view of gene
216 expression changes across the entire homogenized tissue, spatial transcriptomics offers a
217 targeted approach focusing on localized gene expression patterns within distinct regions of
218 interest, such as the endometrium-like structures of lesions. This targeted approach resulted in
219 comparatively few DEG, indicating that the high difference in transcriptomic profiles between
220 lesions and eutopic endometrium found in bulk RNA-seq may not be attributable to endometrium-
221 like tissue in lesions but from the peripheral tissue. This highlights the importance of spatially
222 resolved data in heterogenous tissues like endometriotic lesions. For example, we expect many
223 of the DEG identified in bulk RNA-seq originate from the fibrotic regions of lesions and reflect
224 sustained inflammation and the presence of activated fibroblasts [9, 16]. Interestingly, our findings
225 suggest that the sub-epithelial stroma in superficial peritoneal lesions remains largely unaltered
226 and could serve as an internal control for future spatial experiments, bypassing the requirement
227 for matched eutopic stromal tissue. The paired design of this study increased power with a limited

228 sample size. However, the lack of healthy control endometrium and unknown time since symptom
229 onset are notable caveats and may limit the generalizability of the findings, particularly for the
230 initiation of disease. As such, further research is necessary to elucidate the molecular
231 mechanisms underlying the early pathogenesis of superficial peritoneal endometriosis.

232 The spatial transcriptomic technique, sequencing hybridized probes from specific areas of
233 FFPE tissue, resulted in an overall reduced transcriptome size after removing genes with low
234 counts across segments. The spatial transcriptome included 7,945 genes while the bulk RNA-
235 sequencing analysis included 17,405 genes. Consequently, many of the lowest expression genes
236 from the bulk RNA-sequencing data were filtered from the spatial transcriptome before DEG
237 analysis. The advantage of spatial transcriptomics, however, is gaining information from genes
238 expressed only by a subset of cells or a single cell type that would be lost in the bulk tissue. This
239 is evidenced by the inclusion of 551 genes in the spatial transcriptome that were considered as
240 not expressed in the bulk RNA-sequencing analysis. Further, spatial transcriptomics indicated
241 increased proliferation of the lesion epithelium while bulk RNA-sequencing found an overall
242 reduction in cell cycle gene sets. The epithelium of lesions is likely to be a minor contributor to
243 gene expression from homogenized tissue since lesions often have little or even no remaining
244 epithelial component. Interestingly, these results suggest the lesion epithelium may proliferate in
245 response to inflammatory peritoneal environment while stroma reduces proliferation and may
246 even become senescent [46] . A growing body of evidence has found that senescence plays a
247 role in multiple pathologies and may contribute to endometriotic lesions [47-49].

248 Receptor-ligand analysis identified an almost four-fold increase in signaling between
249 epithelium and macrophages in lesions compared to the endometrium, including multiple
250 inflammatory pathways. MHC-II ligands expressed in the lesion epithelium were predicted to
251 communicate to macrophages through the CD4 receptor. Notably, human monocytes and
252 macrophages express CD4, unlike the mouse, serving as an important target for HIV-1 infection
253 [50-52]. The canonical macrophage marker from this study, CD68, is expressed by monocytes

254 and macrophages [53]. Although monocytes rapidly differentiate into macrophages within a tissue,
255 some monocytes were likely included in the spatial transcriptome analysis. Canonically, MHC-II
256 binding of the CD4 receptor on monocytes promotes differentiation into macrophages [51], thus
257 increased MHC-II in the lesion epithelium would drive macrophage differentiation from circulating
258 monocytes homing to areas of hypoxia and inflammation. Increased expression of MHC class II
259 expression in the epithelium aligns with recent single cell RNA-sequencing analysis of ovarian
260 endometriosis, which found increased MHC class II expression in the epithelium [54].

261 Macrophage migration inhibitory factor (MIF) is constitutively expressed by many cell
262 types and has pleiotropic autocrine and paracrine proinflammatory effects on tissues [55]. MIF
263 signaling in macrophages sustains proinflammatory function by inhibiting apoptosis,
264 counteracting the immunosuppressive effects of glucocorticoids, and promoting secretion of
265 prostaglandin E2 [55, 56]. Additionally, MIF is released by monocytes, macrophages, and other
266 immune cells upon exposure to proinflammatory mediators, such as C3, to reinforce a local
267 proinflammatory environment [57-59].

268 *Complement 3* expression was increased in bulk RNA-sequencing results (3.7-fold, FDR
269 $p = 0.0003$) and found in the lesion epithelium from spatial transcriptomic analysis (4.6-fold, FDR
270 $p = 0.003$). Endometriotic lesions were originally reported to express Complement 3 (C3) by
271 Weed and Arquembourg in 1980 [60] and later found to be secreted by the lesion epithelium [61,
272 62]. In fact, serum levels of C3 are elevated in patients with endometriosis and C3 was proposed
273 as a potential diagnostic biomarker [63]. The complement system is a signaling cascade that plays
274 a pleiotropic role in immune response, including production of proinflammatory mediators and
275 recognition and clearance of pathogens by lysis and enhanced phagocytic uptake by immune
276 cells [64]. The cascade of over 50 proteins is characterized by a series of protein cleavage events
277 that produce inflammatory cytokines and the components for subsequent steps. Multiple stimuli
278 can activate the complement system, but all pathways converge on activation of C3 by a
279 convertase. Although the presence of C3 in endometriotic lesions has been known for 40 years,

280 its potential contribution to the disease is unclear [65]. Following cleavage, the resulting fragments
281 are referred to by appending the letter “a”, for the smaller fragment, or “b”, for the larger fragment,
282 to the protein name, for example, C3a.

283 C3a and C3b are produced following activation of C3 by a C3 convertase, itself the product
284 of prior cleavage events. C3b induces phagocytic activity of macrophages, but lesion tissue is
285 refractory to complement targeting through multiple mechanisms. CD47, otherwise known as the
286 “don’t eat me signal”, is expressed by tissue and binds to the SIRPα receptor on macrophages,
287 inhibiting phagocytosis [66, 67]. Complement regulatory proteins, such as CD35, CD46, and
288 CD55, inhibit complement attack by accelerating breakdown or direct cleavage of complement
289 components critical for continuation of the cascade [64]. In the event of complement activation,
290 CD59, another complement regulatory protein, inhibits formation of the membrane attack complex
291 and prevents cell lysis [68]. Thus, multiple mechanisms exist within the lesion to prevent direct
292 complement attack but complement signaling promotes a localized proinflammatory environment.

293 The proinflammatory cytokine C3a, released following C3 cleavage, can activate a pro-
294 repair or tumor-associated macrophage (TAM) phenotype by binding to C3AR1, as found in the
295 ligand-receptor analysis [69]. This provides a mechanism by which C3 activation from the
296 superficial peritoneal endometriotic lesion epithelium promotes the pro-lesion macrophage
297 phenotype described as pro-repair, tumor-associated, or M2. These macrophages then contribute
298 to lesion tissue remodeling including neovascularization and fibrosis [18, 70, 71]. Additionally,
299 semaphorin 3B was found in the lesion epithelium signaling to macrophages and could further
300 promote the pro-disease TAM phenotype since SEMA3B increased expression of pro-repair
301 macrophage markers in a model of rheumatoid arthritis [72].

302 Activated complement signaling in tissue induces a diffuse inflammatory state that
303 includes increased prostaglandins, also upregulated by MIF [PMID: 33505394]. Increased
304 prostaglandins can activate steroidogenic enzymes and, potentially the production of estradiol
305 and estrone by the lesion [31, 33, 35, 73]. Finally, increased estrogens can activate complement

306 in lesion tissue [74] resulting a positive feedback loop, common in pathogenic signaling. In this
307 manner, the complement signaling is sustained by local estrogenic activity and could sustain local
308 inflammation and the presence of pro-repair macrophages until such time as the lesion becomes
309 completely fibrotic with a tissue stiffness that no longer supports cell growth and the lesion
310 becomes scar tissue and contributes to peritoneal adhesions. In support of complement signaling
311 promoting lesion pathogenesis, C3 null uterine tissue formed fewer lesions after 21 days in a
312 mouse model of endometriosis [75].

313 The comparison of lesions to eutopic endometrium yielded intriguing insights into the
314 molecular and cellular dynamics underlying lesion pathophysiology. Firstly, despite previous
315 findings from bulk tissue analysis suggesting significant differences between endometrium-like
316 tissue in lesions and eutopic endometrium, our spatial transcriptomic data reveal a surprising
317 similarity between these two tissues. The lack of drastic differences may be attributed to the
318 composition of the excised lesions used in bulk RNA-sequencing, with endometrium-like tissue
319 comprising only a small proportion of the lesion, such that differential expression was largely
320 attributable to the peripheral stroma and fibrotic tissue. Notably, this difference highlights the
321 importance of employing advanced techniques, like spatial transcriptomics, to gain an improved
322 understanding of lesion biology.

323 Secondly, spatial transcriptomics has provided novel insights into the intricate cellular
324 crosstalk within lesions. Our data indicate signaling between the stroma and epithelium, as well
325 as between the lesion epithelium and macrophages. Notably, the epithelium emerged as a central
326 player in driving inflammation within the lesion, promoting inflammatory signaling independent of
327 the stromal compartment. Moreover, the presence of CD68+ cells amid epithelial cells highlights
328 the physiological relevance of cell-cell interactions across different cell types.

329 Drawing from these observations, we present a model wherein the superficial lesion
330 epithelium orchestrates inflammatory signaling within the lesion while promoting a pro-repair
331 phenotype in infiltrating macrophages. Spatial transcriptomics facilitated the identification of

332 inflammatory signaling emanating from the epithelium, including C3, MIF, and MHC class II. This
333 novel insight sheds light on the pathological consequence of C3 expressed by the epithelium in
334 modulating macrophage phenotype to support lesion development. In summary, our study
335 underscores the critical role of considering spatial context and cellular interactions within lesions
336 to unravel the complexities of superficial peritoneal endometriotic lesions. Further investigation is
337 imperative to elucidate the specific mechanisms governing epithelium-driven inflammation and its
338 implications for disease progression and therapeutic interventions.
339

340 # Methods

341 ## Human Tissues

342 All protocols involving tissue collection were approved by the institutional review board
343 (IRB) Committee of Ponce Health Sciences University, School of Medicine (PHSU). Endometriotic
344 lesions and matched eutopic uterine tissues from 10 patients were obtained as archived
345 deidentified formalin-fixed paraffin-embedded (FFPE) tissue blocks [76-78]. All tissues were
346 previously evaluated by a pathologist to confirm the diagnosis of endometriosis and menstrual
347 cycle stage of eutopic endometrium using Noyes criteria [79].

348 ## Histology

349 Tissue blocks were sectioned and trichrome stained (StatLab #KTTRBPT) to confirm the
350 presence of defined epithelial and stromal compartments in lesions. Blocks were serial sectioned
351 at 6 μm thickness and floated onto positively charged microscope slides. Tissues were attached
352 to the slides prior to processing by heating on a slide warmer for 15 minutes. Tissues were then
353 deparaffinized and rehydrated through three changes each of xylenes for five minutes and 100%
354 ethanol for one minute before a rinsing in running tap water for one minute. Slides were incubated
355 in Bouin's fluid at room temperature overnight. Slides were rinsed in running tap water for three
356 minutes and immersed in modified Mayer's hematoxylin stain for four minutes at room

357 temperature. After a three-minute rinse in running tap water, slides were immersed in one step
358 trichrome stain for five minutes and rinsed in running tap water for five seconds. Slides were then
359 dehydrated through three changes of 100% ethanol for one minute, cleared in three changes of
360 xylenes for one minute, and a coverslip was applied with Permount mounting medium (Fisher
361 Scientific #SP15).

362 ## Spatial Transcriptomics

363 Human tissue slide preparation, library generation, and sequencing for digital spatial
364 profiling (DSP) on the nanoString GeoMx DSP instrument were performed by the Van Andel
365 Institute Histology and Genomics Cores. Sections were cut at 5 μm thickness and mounted on
366 plus-charged slides (Epredia Colormark Plus #CM-4951WPLUS-001). Slides were baked at 60°C
367 for one hour and stored at 4°C in a vacuum-sealed container containing desiccant for up to two
368 weeks. All subsequent steps were performed under RNase-free conditions with DEPC-treated
369 water. Slides were deparaffinized with three sequential five-minute washes in xylenes, followed
370 by two washes in 100% ethanol for five minutes, one wash in 95% ethanol, and one wash in 1X
371 PBS. Antigen retrieval was performed in target retrieval reagent (EDTA, pH 9.0; Invitrogen #00-
372 4956-58) diluted to 1X in the BioGenex EZ-Retriever System for 10 minutes at 95°C. Slides were
373 then washed with 1X PBS for five minutes. Slides were then incubated in 1 μg/mL proteinase K
374 10 minutes at 37°C and washed in 1X PBS for five minutes at room temperature. Slides were
375 fixed for five minutes in 10% neutral buffered formalin followed by two washes in NBF stop buffer,
376 for five minutes each, and one wash in 1X PBS for five minutes. Slides were then incubated with
377 UV-photocleavable Human Whole Transcriptome Atlas hybridization probes diluted in buffer R
378 (GeoMx RNA Slide Prep FFPE-PCLN kit, #121300313) in a hybridization oven at 37°C for 16-20
379 hours. Following probe incubation, slides were washed with stringent buffer (1:1, formamide:4X
380 SSC buffer; Thermo Fisher #AM9342; Sigma-Aldrich #S6639) at 37°C twice for 25 minutes each.
381 Then slides were washed twice in 2X SSC buffer. Slides were blocked in 200 μL buffer W (GeoMx

382 RNA Slide Prep FFPE-PCLN kit) for 30 minutes and incubated at 4ºC overnight with SYTO 13
383 nucleic acid stain (500 nM; Thermo Fisher Scientific #S7575) and antibodies for pan-cytokeratin
384 (panCK; 1 µg/mL; Novus Biologicals #NBP2-33200AF488), smooth muscle actin (ACTA2; 1.25
385 µg/mL; Abcam #ab202368), and CD68 (0.5 µg/mL; Santa Cruz Biotechnology #sc-20060AF647)
386 diluted in buffer W. Slides were washed four times in 2X SSC buffer for 3 minutes each and placed
387 in the nanoString GeoMx DSP instrument.

388 Duplicate 500 μm^2 regions of interest (ROI) were selected for each based on fluorescent
389 imaging on the GeoMx DSP instrument (nanoString Technologies). ROI were drawn in the central
390 portion of the endometrium stratum functionalis, to include glandular and not luminal epithelium,
391 for eutopic uterine tissue and in lesions areas with defined epithelium. ROIs were then segmented
392 in order of macrophages (CD68+), epithelium (panCK+), and stroma (ACTA2-) areas of
393 illumination (AOI) for individual collection. AOI were processed sequentially on the instrument
394 using UV light focused through each AOI that released the photocleavable oligos into wells of a
395 96 well plate. After AOI collection, indexing primers were hybridized during nanoString library
396 preparation. Quality and quantity of the finished library pools were assessed using a combination
397 of Agilent DNA High Sensitivity chips (Agilent Technologies, Inc.) and the QuantiFluor dsDNA
398 System (Promega Corp.). Paired end, 50 bp sequencing was performed on an Illumina Novaseq
399 6000 sequencer using an S2, 100 cycle sequencing kit v1.5 (Illumina Inc.). Basecalling was done
400 by Illumina RTA3 and output was demultiplexed and converted to fastq format with bcl2fastq
401 v1.9.0.

402 Spatial Data Analysis

403 Fastq files were converted to digital count conversion (DCC) files using GeoMx NGS
404 Pipeline v2.3.3.10. Sample annotation, PKC configuration, and DCC files were imported with
405 GeomxTools (v3.2.0) in R to generate a NanoStringGeoMxSet object. Read counts with a value
406 of zero were shifted to one for downstream transformations and quality control (QC) analyses.

407 Each AOI, or segment, was assessed for sequencing and tissue quality. Outlier probes were then
408 excluded before counts were collapsed to gene-level data (18,677 genes) by geometric mean.
409 The limit of quantification (LOQ) was determined per segment based on the distribution of
410 negative control probes and set at two geometric standard deviations above the geometric mean
411 with a minimum value of two. Segments with a gene detection rate less than 10% were filtered
412 before removing genes detected in less than 10% of segments. Separation between the upper
413 quartile 3 (Q3) of gene counts and the geometric mean of the negative probes was confirmed
414 before count normalization using the quartile 3 (Q3) method.

415 Normalized read counts were $\log_2$-transformed and dimension reduction was performed
416 by uniform manifold approximation and projection (UMAP) [80] with the umap package (v0.2.10)
417 with the random state set to 42. Differential expression analyses were completed using $\log_2$-
418 transformed normalized read counts with a linear model approach in the limma package (v3.54.2).
419 A linear model was fit for each gene with lmFit before an empirical Bayes test was completed
420 using patient as a covariate. P-values were corrected for multiple testing with the Benjamini
421 Hochberg method included in the decideTests function of limma. Genes were considered
422 differentially expressed when the adjusted p-value was below 0.05. Principal component analysis,
423 volcano plots, gene set enrichment analysis, and over-representation tests were completed as
424 described for bulk RNA-sequencing data.

425 Bulk RNA-sequencing Analysis

426 Read counts per gene were downloaded from eutopic endometrium (n = 7) and peritoneal
427 endometriotic lesion samples (n = 6) for series GSE179640 [21] from the NCBI Gene Expression
428 Omnibus repository. Files were parsed with R (version 4.2.0) and all subsequent analyses, unless
429 otherwise noted, were completed in R using RStudio [81]. Differential expression analysis was
430 conducted using the edgeR-robust method (v4.0.3) [82]. Genes with low counts per million (CPM)
431 were removed using the filterByExpr function from edgeR. Multidimensional scaling plots,

432 generated with the plotMDS function of edgeR, were used to investigate group separation prior
433 to statistical analysis. Principal component analysis of normalized log_2-transformed CPM was
434 conducted with the PCAtools package (v2.10). The biplot and pairsplot functions were used to
435 visualize sample separation across principal components one through five. Differentially
436 expressed genes (DEG) were identified based on Benjamini-Hochberg false discovery rate (FDR)
437 p-values less than 0.05. The hclust function was used for hierarchical clustering (ward.D2) of
438 Euclidean distances and plotted with the dendextend package (v1.17.1). A volcano plot was
439 generated with EnhancedVolcano (v1.16) and the top 20 DEG, based on FDR p-value, were
440 labeled. Gene set enrichment and over-representation analyses were completed with
441 clusterProfiler package (version 4.6.0) using mSigDB reference databases.

442 Receptor-Ligand Analysis

443 Quantile-normalized read counts were used for receptor-ligand analysis with the CellChat
444 package (1.6.10) in R [29]. Significant genes and interactions were identified using the functions
445 `identifyOverExpressedGenes` and `identifyOverExpressedInteractions`. Communication
446 probabilities were calculated between cell types with raw input counts option enabled, as
447 recommended for bulk-sequencing data. The resulting interactions were visualized using the
448 included plotting functions. Weighted communication probabilities were subset for eutopic
449 endometrium or lesions before calculating tissue-specific communication interaction strengths.

450 # Figures

Figure 1

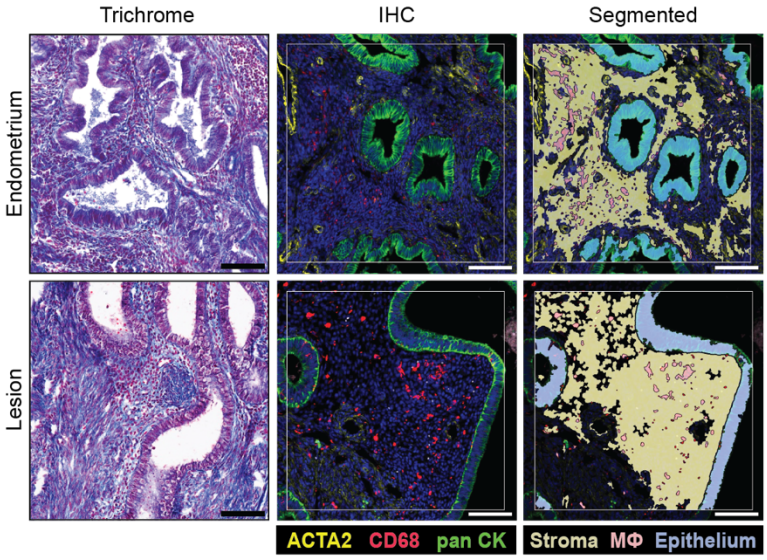

451 ## Figure 1

452 Segmentation strategy for spatial transcriptomics. Superficial peritoneal endometriotic lesions and
453 matched endometrium (n = 10) were visualized with trichrome staining to confirm the presence of
454 epithelial and stromal compartments. Tissues were immunostained for pan-cytokeratin, CD68,
455 and ACTA2 for segmentation and spatial transcriptome collection on the GeoMx platform.
456 Representative regions of interest (ROI) are shown for each tissue type. Duplicate ROI were
457 collected for each tissue and stroma, epithelium, and macrophages were segmented from each
458 for a total of 20 ROI and 60 segments. Scale bar = 100 μm.

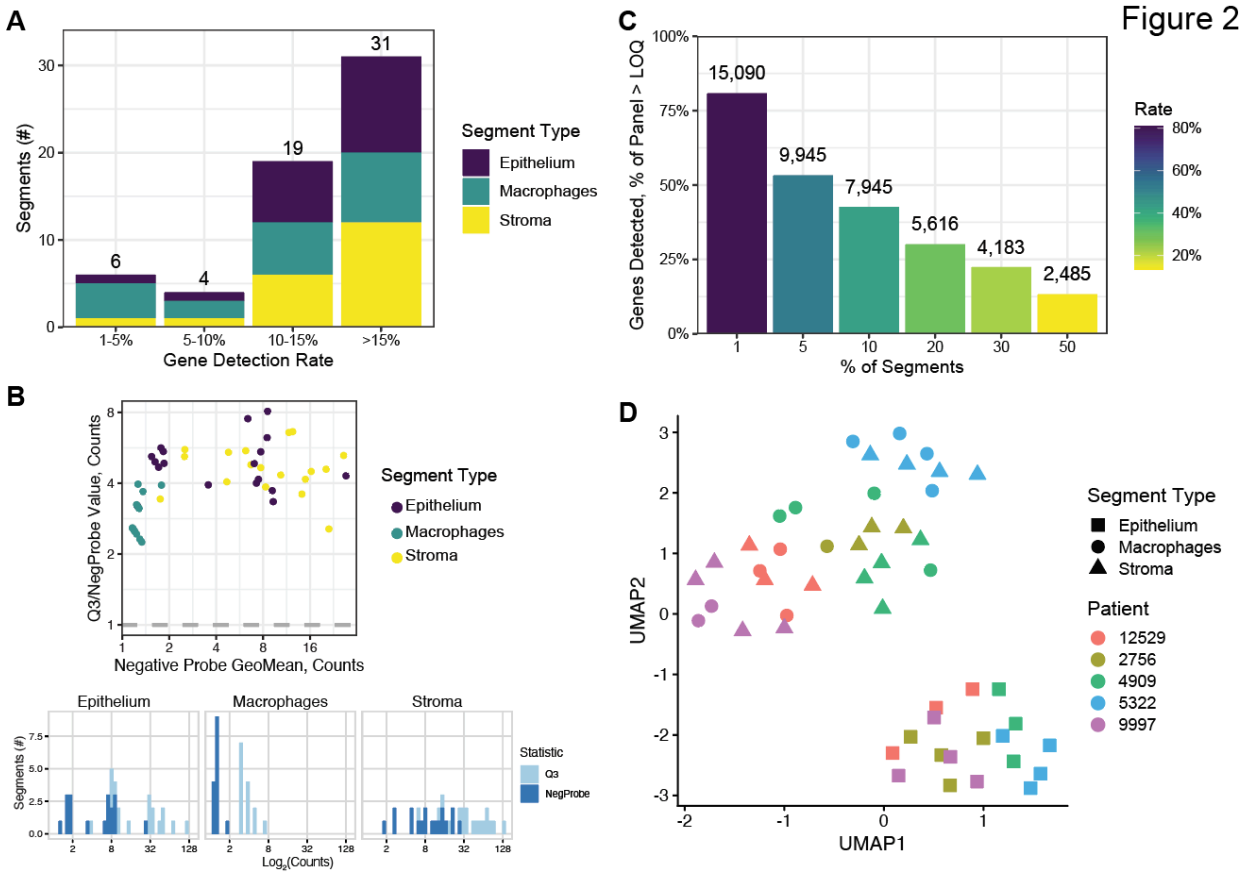

Figure 2

Spatial transcriptomics results from eutopic endometrium superficial peritoneal endometriotic lesions. (A) Bar plot of all 60 segments separated by gene detection rate. Segments with a rate of less than 10% were removed. (B) Confirmation of effective count normalization by separation of the gene counts and negative probe counts in a scatter plot and separation of count distributions by cell type. (C) Bar plot of detectable genes per segment used for filtering genes found in less than 10% of segments leaving 7,945 genes for further analysis. (D) Dimensionality reduction UMAP plot of all segments coded by shape and colored by patient. Epithelium clustered separately from stroma and macrophages.

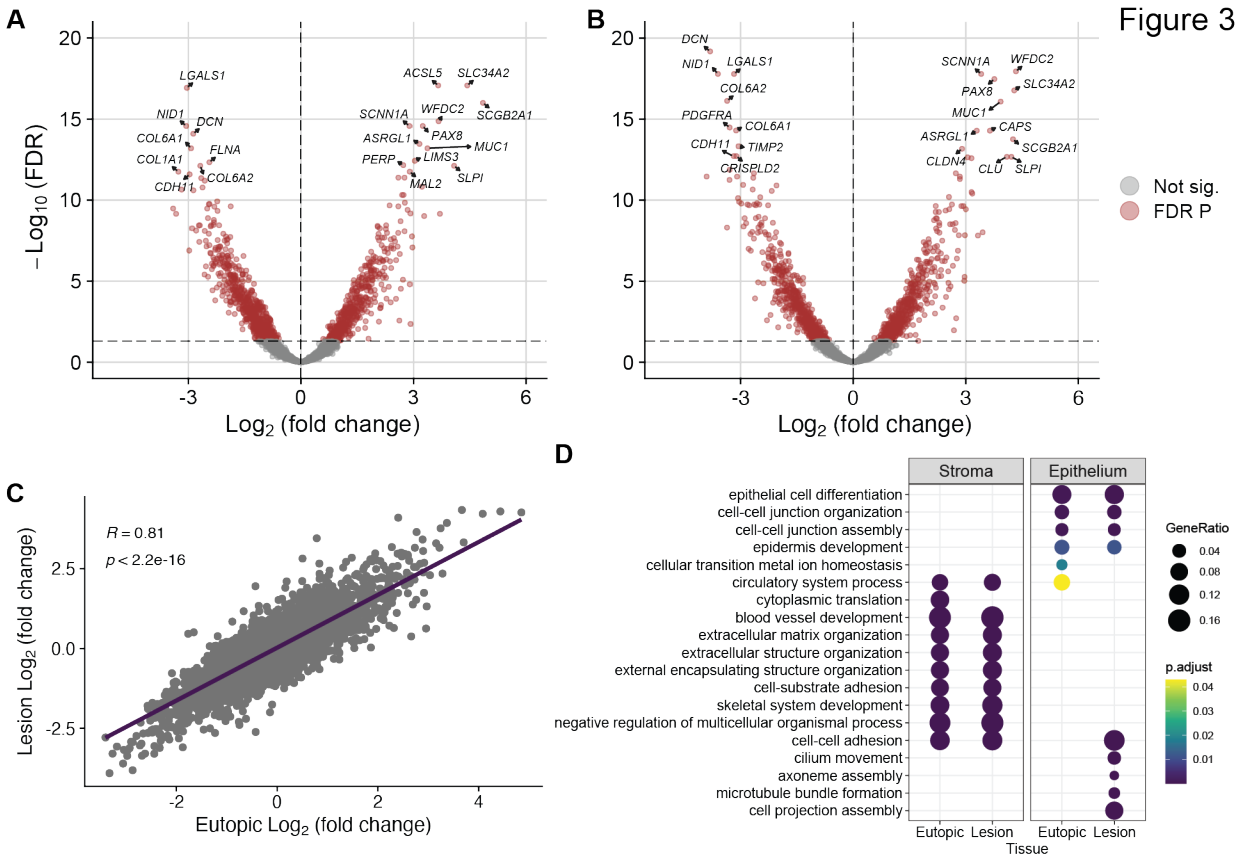

Figure 3

Epithelium versus stroma in eutopic endometrium and lesions. Volcano plots of differentially expressed genes (DEG) in the (A) endometrium and (B) lesions. The top DEG were similar in volcano plots with canonical epithelial genes like *MUC1*, *PAX8*, and *WFDC2* increased in both epithelia. (C) Genes enriched for each compartment were highly correlated in the eutopic endometrium and lesions. (D) Enriched gene ontology biological process terms were consistent with cell type, including extracellular matrix genes in the stroma and cell-cell junction genes in the epithelium, in the eutopic endometrium and lesions. Several terms related to cell-projections and cilia were unique, however, to the lesion epithelium.

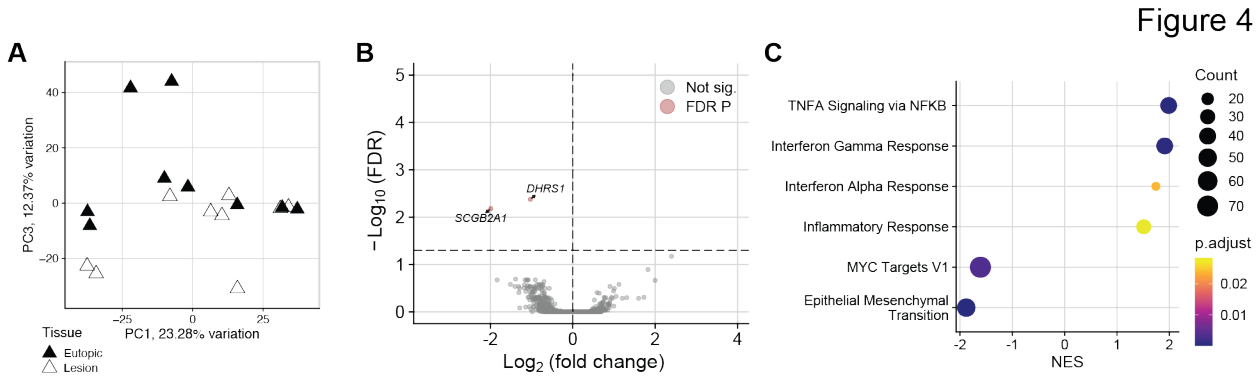

Figure 4

Endometriotic sub-epithelial stroma is minimally altered compared to eutopic endometrium. (A) Principal component (PC) plot of lesion stroma compared to eutopic endometrium showed group separation most clearly on PC3. (B) Volcano plot of two down-regulated genes in the endometriotic stroma. (C) Gene set enrichment analysis of hallmark pathways found four increased inflammatory gene sets and two decreased.

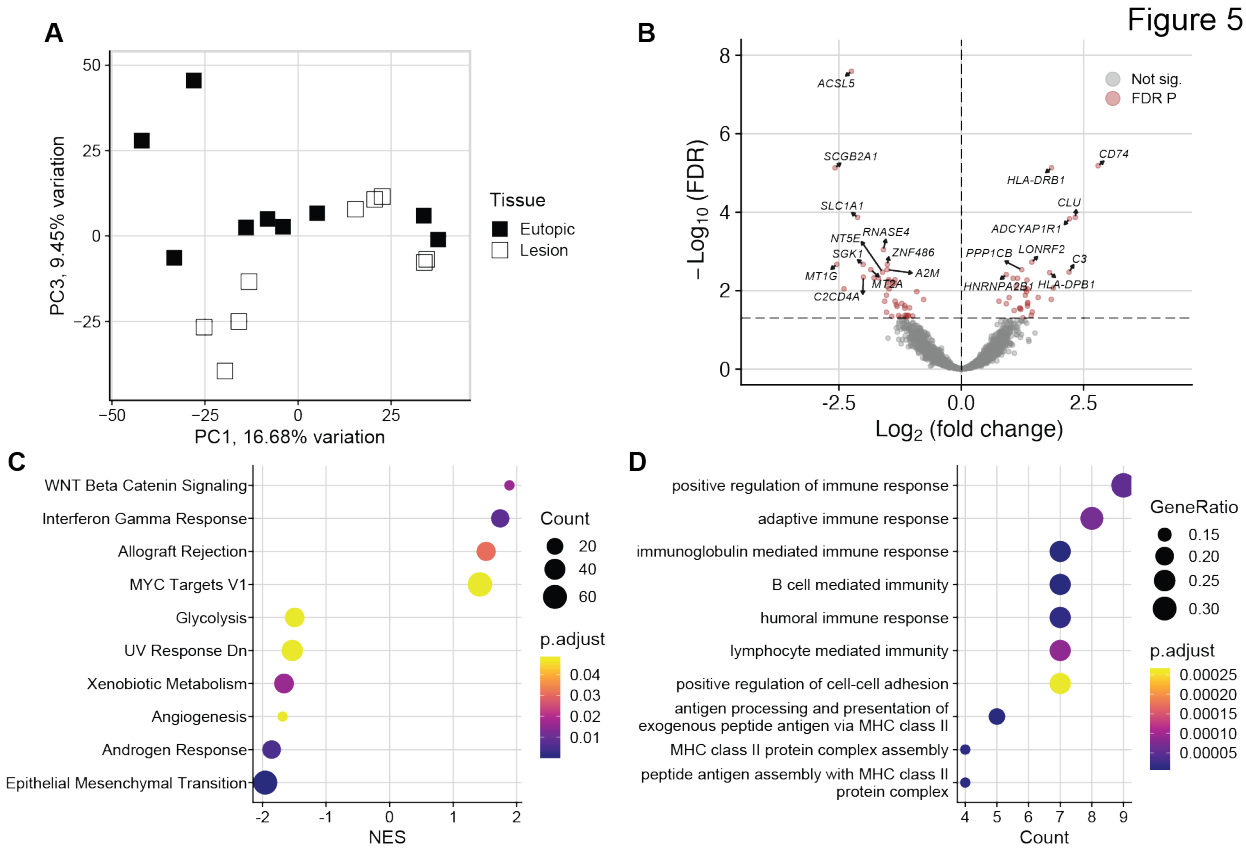

Figure 5

Immune response genes are increased in the endometriotic lesion epithelium. (A) Principal component (PC) plot of lesion epithelium compared to eutopic endometrium showed group separation most clearly on PC3. (B) Volcano plot of 76 differentially expressed genes (DEG) in the endometriotic epithelium. Of note, complement 3, *C3*, was one of the top increased DEG and several others were major histocompatibility complex class II related genes, like *CD74* and *HLA-DRB1*. (C) Gene set enrichment analysis of hallmark pathways found four increased gene sets and six decreased, indicating increased inflammation and proliferation. (D) Nine of the top 10 enriched gene ontology biological process terms were immune related.

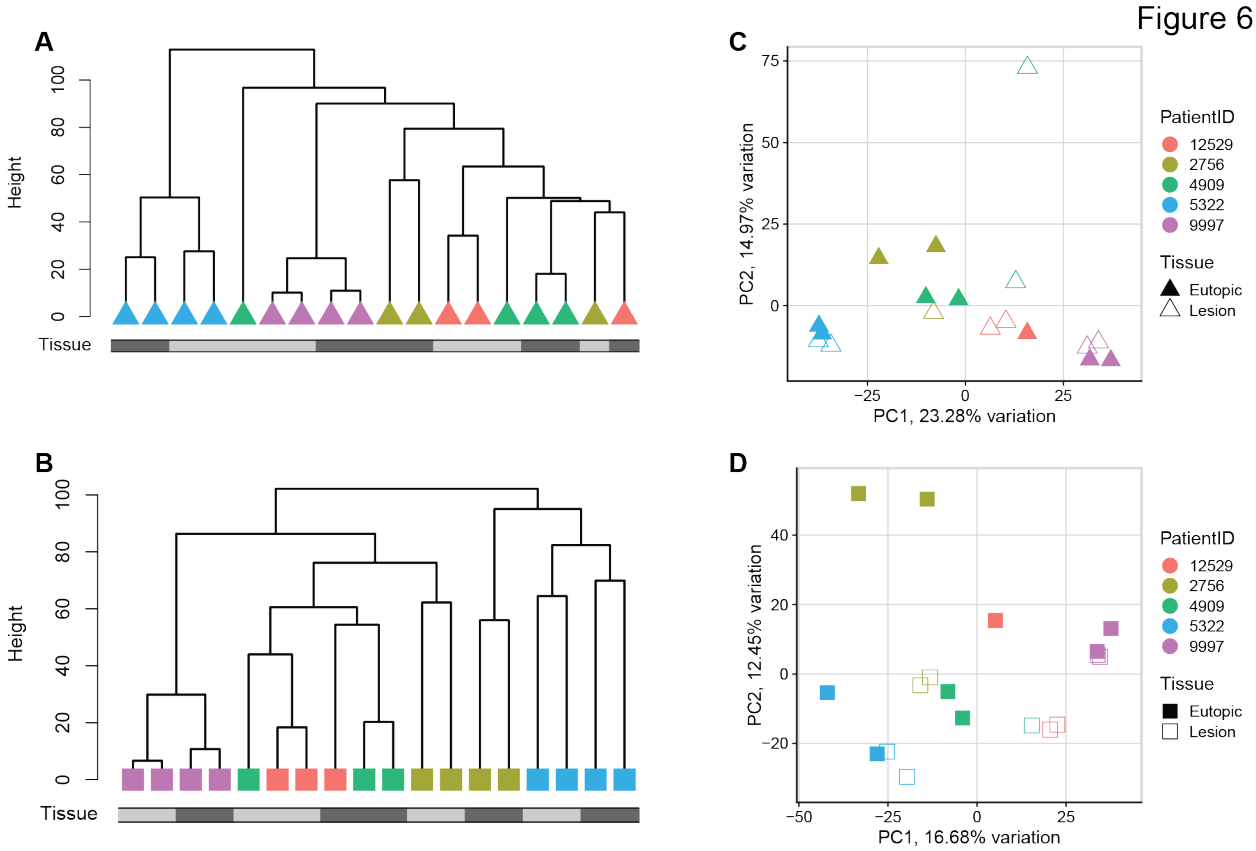

Figure 6

Neither stroma nor epithelium cluster by lesion versus eutopic endometrium. Hierarchical clustering dendrograms of (A) stroma and (B) epithelium segments found no clustering of segments by tissue of origin (endometrium = black bar). Principal component (PC) plots demonstrated that PC1, the largest component of variation, was correlated with patient identity.

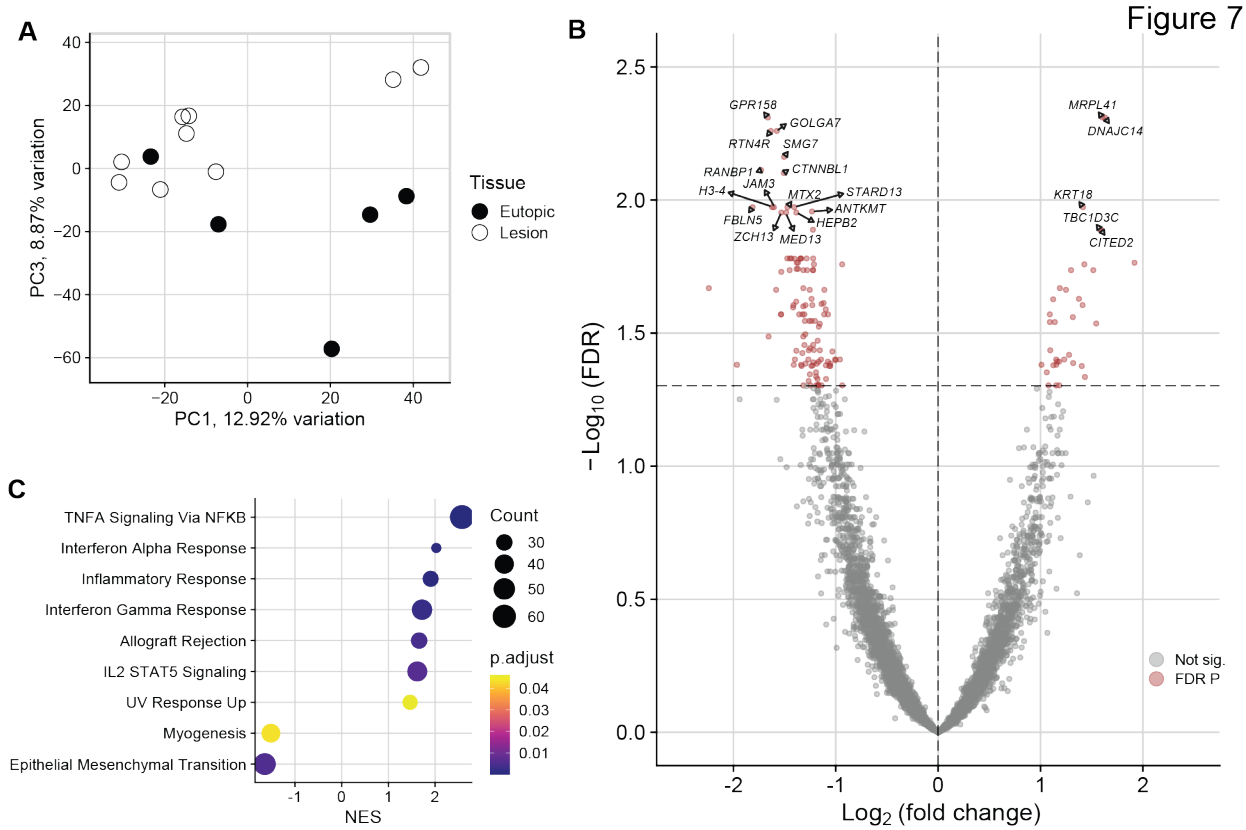

Figure 7

Macrophages are altered in endometriotic lesions. A) Principal component (PC) plot of lesion macrophages compared to eutopic endometrium showed group separation most clearly on PC3. (B) Volcano plot of 148 differentially expressed genes (DEG) in the endometriotic macrophages. (C) Gene set enrichment analysis of hallmark pathways found seven increased gene sets and two decreased, indicating increased inflammation likely reflective of the presence of monocyte-derived macrophages in the lesion tissue.

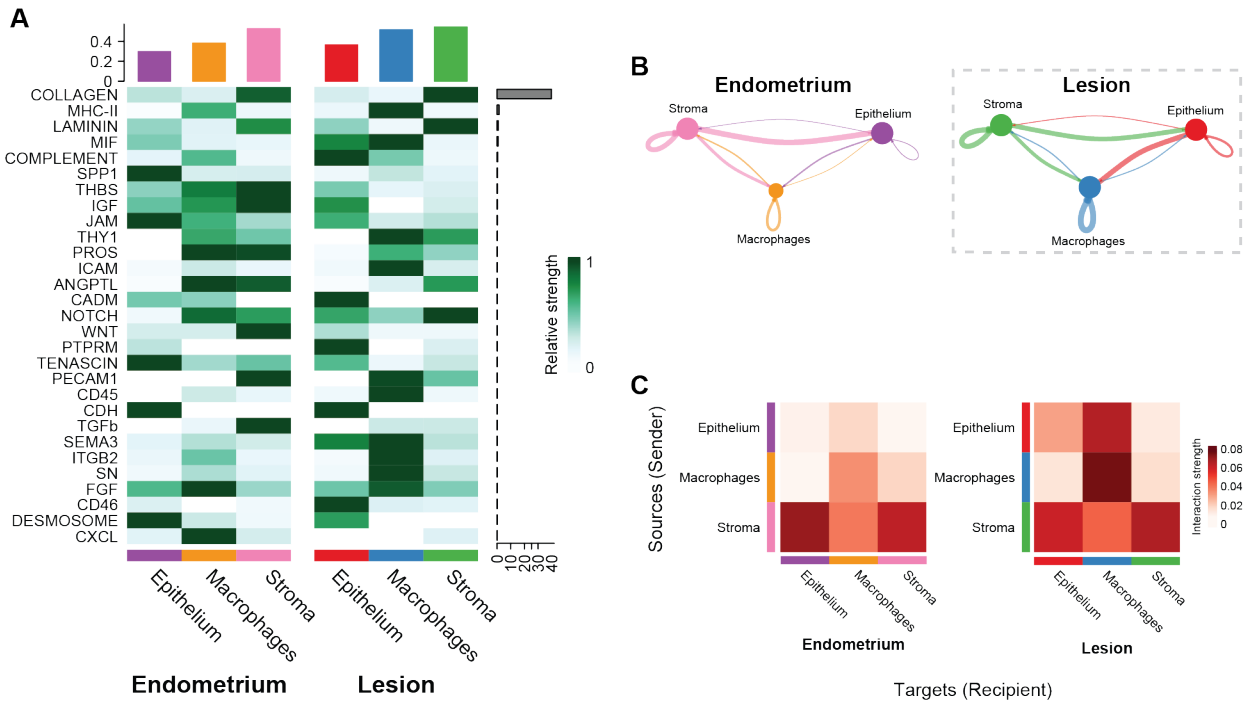

Figure 8

CellChat ligand-receptor analysis identified increased communication from the lesion epithelium to macrophages. (A) Signaling pathway heatmap of all 29 significant pathways identified by CellChat sorted by signaling strength, indicated by the gray bar. Interactions, combined incoming and outgoing, totaled for each cell type in the bar plot at the top of the heatmap and scaled per row. (B) Circle plots of communication networks including 24 pathways in the endometrium and 26 in lesions where line thickness corresponds to strength. Stroma to epithelium communication was strong in the eutopic endometrium and similarly present in the lesions. However, epithelium to macrophage communication was increased 3.7-fold in lesions. (C) Interaction strength heatmaps highlight the gain of epithelium to macrophage signals in lesions and strong macrophage-macrophage interactions.

Figure 9

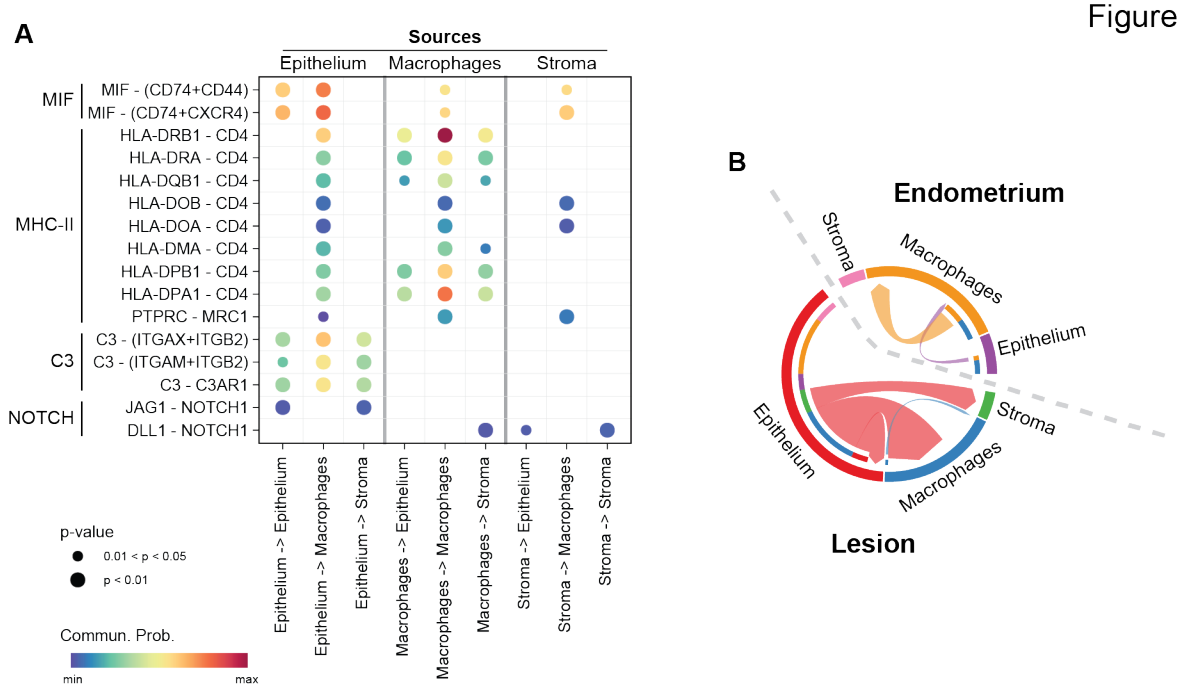

Figure 9

Inflammatory ligands originate in the endometriotic lesion epithelium. (A) Ligand – receptor dot plot of inflammatory pathways in endometriotic lesions. Pathway names are indicated on the left side of the plot followed by specific ligand and receptor interactions. All signals originating from the lesion epithelium are in the left three columns, macrophages in the center, and stroma on the right. Complement and major histocompatibility complex class II (MHC-II) pathways originated in the lesion epithelium and not the stroma. Macrophage migration inhibitory factor (MIF) signaling was strongest in the epithelium, but also sent from the stroma and macrophage cell types. (B) Complement signaling chord diagram of the weighted complement signaling pathway indicating increased signaling from the lesion epithelium compared to the eutopic endometrium epithelium.

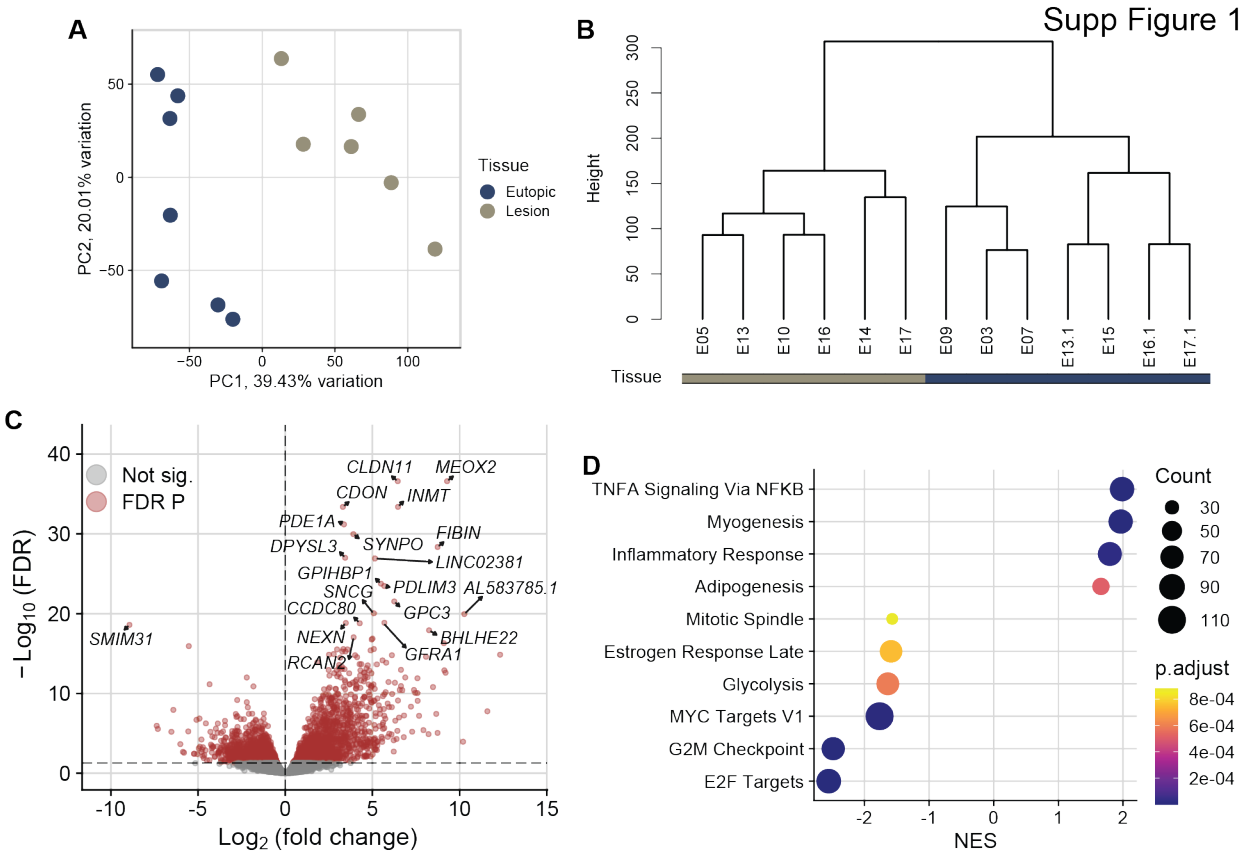

Supplemental Figure 1

Transcriptome alterations in superficial endometriotic lesions compared to eutopic endometrium as measured by bulk RNA-sequencing. (A) Principal component (PC) plot of superficial peritoneal endometriotic lesions and eutopic endometrium (n = 13) from GSE179640. Samples were separated across PC1 by tissue type, representing 39% of variation in gene expression. (B) Hierarchical clustering dendrogram confirmed separation of lesions from eutopic endometrium. (C) Volcano plot of 3,656 differentially expressed genes in lesions versus endometrium. (D) Gene set enrichment analysis of hallmark pathways found inflammation, represented by TNFα signaling via NF-κB and inflammatory response, increased in lesions while three cell cycle-related gene sets, MYC targets, G2M checkpoint, and E2F targets were decreased. This indicates increased inflammation and decreased proliferation in lesions compared to eutopic endometrium.

541 Table 1

542 Patient demographics, indications for surgery, and post-operative diagnosis.

Patient	Age	Indication(s)	Diagnosis
2756	47	Uterine Leiomyoma Adenomyosis	Endometriosis L ovary and oviduct
4909	36	Uterine Leiomyoma Pelvic pain	Endometriosis, Leiomyoma
5322	49	Uterine Leiomyoma	Endometriosis L&R ovary, Leiomyoma
9997	36	Pelvic pain	Endometriosis R oviduct, Endometrioma L ovary, Pelvic adhesions
12529	44	Uterine Leiomyoma	Endometriosis L&R oviduct, Leiomyoma

543

544 # References

545 1. Eskenazi B, Warner ML. Epidemiology of endometriosis. Obstet Gynecol Clin North Am.
546 1997;24(2):235-58. Epub 1997/06/01. PubMed PMID: 9163765.
547 2. Bulun SE. Endometriosis. N Engl J Med. 2009;360(3):268-79. Epub 2009/01/16. doi:
548 10.1056/NEJMra0804690. PubMed PMID: 19144942.
549 3. Giudice LC. Clinical practice. Endometriosis. N Engl J Med. 2010;362(25):2389-98. Epub
550 2010/06/25. doi: 10.1056/NEJMcp1000274. PubMed PMID: 20573927; PubMed Central
551 PMCID: PMCPMC3108065.
552 4. Practice Committee of the American Society for Reproductive Medicine. Treatment of pelvic
553 pain associated with endometriosis. Fertil Steril. 2008;90(5 Suppl):S260-9. Epub 2008/11/26.
554 doi: 10.1016/j.fertnstert.2008.08.057. PubMed PMID: 19007642.
555 5. Endometriosis and infertility: a committee opinion. Fertil Steril. 2012;98(3):591-8. Epub
556 2012/06/19. doi: 10.1016/j.fertnstert.2012.05.031. PubMed PMID: 22704630.
557 6. Koninckx PR, Martin DC. Deep endometriosis: a consequence of infiltration or retraction or
558 possibly adenomyosis externa? Fertil Steril. 1992;58(5):924-8. Epub 1992/11/01. doi:
559 10.1016/s0015-0282(16)55436-3. PubMed PMID: 1426377.
560 7. Koninckx PR, Ussia A, Adamyan L, Wattiez A, Donnez J. Deep endometriosis: definition,
561 diagnosis, and treatment. Fertil Steril. 2012;98(3):564-71. Epub 2012/09/04. doi:
562 10.1016/j.fertnstert.2012.07.1061. PubMed PMID: 22938769.
563 8. Sampson JA. Peritoneal endometriosis due to the menstrual dissemination of endometrial
564 tissue into the peritoneal cavity. American Journal of Obstetrics & Gynecology.
565 1927;14(4):422-69. doi: 10.1016/S0002-9378(15)30003-X.
566 9. Zondervan KT, Becker CM, Koga K, Missmer SA, Taylor RN, Vigano P. Endometriosis. Nat
567 Rev Dis Primers. 2018;4(1):9. Epub 2018/07/22. doi: 10.1038/s41572-018-0008-5. PubMed
568 PMID: 30026507.
569 10. Hastings JM, Fazleabas AT. A baboon model for endometriosis: implications for fertility.
570 Reprod Biol Endocrinol. 2006;4 Suppl 1:S7. Epub 2006/11/23. doi: 10.1186/1477-7827-4-S1-
571 S7. PubMed PMID: 17118171; PubMed Central PMCID: PMCPMC1775067.
572 11. Jones CJ, Denton J, Fazleabas AT. Morphological and glycosylation changes associated with
573 the endometrium and ectopic lesions in a baboon model of endometriosis. Hum Reprod.
574 2006;21(12):3068-80. Epub 2006/10/05. doi: 10.1093/humrep/del310. PubMed PMID:
575 17018533.

576 12. Harirchian P, Gashaw I, Lipskind ST, Braundmeier AG, Hastings JM, Olson MR, et al. Lesion
577 kinetics in a non-human primate model of endometriosis. Hum Reprod. 2012;27(8):2341-51.
578 Epub 2012/06/08. doi: 10.1093/humrep/des196. PubMed PMID: 22674203; PubMed Central
579 PMCID: PMCPMC3398680.
580 13. Greaves E, Cousins FL, Murray A, Esnal-Zufiaurre A, Fassbender A, Horne AW, et al. A novel
581 mouse model of endometriosis mimics human phenotype and reveals insights into the
582 inflammatory contribution of shed endometrium. Am J Pathol. 2014;184(7):1930-9. Epub
583 2014/06/10. doi: 10.1016/j.ajpath.2014.03.011. PubMed PMID: 24910298; PubMed Central
584 PMCID: PMCPMC4076466.
585 14. Dorning A, Dhami P, Panir K, Hogg C, Park E, Ferguson GD, et al. Bioluminescent imaging in
586 induced mouse models of endometriosis reveals differences in four model variations. Dis
587 Model Mech. 2021;14(8). Epub 2021/08/13. doi: 10.1242/dmm.049070. PubMed PMID:
588 34382636; PubMed Central PMCID: PMCPMC8419713.
589 15. Vigano P, Ottolina J, Bartiromo L, Bonavina G, Schimberni M, Villanacci R, et al. Cellular
590 Components Contributing to Fibrosis in Endometriosis: A Literature Review. J Minim Invasive
591 Gynecol. 2020;27(2):287-95. Epub 2019/12/01. doi: 10.1016/j.jmig.2019.11.011. PubMed
592 PMID: 31785417.
593 16. Vigano P, Candiani M, Monno A, Giacomini E, Vercellini P, Somigliana E. Time to redefine
594 endometriosis including its pro-fibrotic nature. Hum Reprod. 2018;33(3):347-52. Epub
595 2017/12/06. doi: 10.1093/humrep/dex354. PubMed PMID: 29206943.
596 17. Brosens I, Puttemans P, Benagiano G. Which cell defines endometriosis? Hum Reprod.
597 2018;33(3):357-60. Epub 2018/02/09. doi: 10.1093/humrep/dey016. PubMed PMID:
598 29420768.
599 18. Capobianco A, Rovere-Querini P. Endometriosis, a disease of the macrophage. Front
600 Immunol. 2013;4:9. Epub 2013/02/02. doi: 10.3389/fimmu.2013.00009. PubMed PMID:
601 23372570; PubMed Central PMCID: PMCPMC3556586.
602 19. Song Y, Burns GW, Joshi NR, Arora R, Kim JJ, Fazleabas AT. Spheroids as a model for
603 endometriotic lesions. JCI Insight. 2023;8(11). Epub 2023/04/27. doi:
604 10.1172/jci.insight.160815. PubMed PMID: 37104033.
605 20. Marla S, Mortlock S, Heinosalo T, Poutanen M, Montgomery GW, McKinnon BD. Gene
606 expression profiles separate endometriosis lesion subtypes and indicate a sensitivity of
607 endometrioma to estrogen suppressive treatments through elevated ESR2 expression. BMC
608 Med. 2023;21(1):460. Epub 2023/11/24. doi: 10.1186/s12916-023-03166-1. PubMed PMID:
609 37996888; PubMed Central PMCID: PMCPMC10666321.

610 21. Tan Y, Flynn WF, Sivajothi S, Luo D, Bozal SB, Davé M, et al. Single-cell analysis of
611 endometriosis reveals a coordinated transcriptional programme driving immunotolerance and
612 angiogenesis across eutopic and ectopic tissues. Nat Cell Biol. 2022. Epub 2022/07/22. doi:
613 10.1038/s41556-022-00961-5. PubMed PMID: 35864314.
614 22. Fonseca MAS, Haro M, Wright KN, Lin X, Abbasi F, Sun J, et al. Single-cell transcriptomic
615 analysis of endometriosis. Nat Genet. 2023;55(2):255-67. Epub 2023/01/10. doi:
616 10.1038/s41588-022-01254-1. PubMed PMID: 36624343.
617 23. Li R, Tran DN, Lessey BA, Young SL, Kim TH, Jeong JW. Transcriptomic changes in eutopic
618 endometrium and ectopic lesions during endometriosis progression in a mouse model. F S
619 Sci. 2024. Epub 2024/02/12. doi: 10.1016/j.xfss.2024.02.001. PubMed PMID: 38342342.
620 24. Zollinger DR, Lingle SE, Sorg K, Beechem JM, Merritt CR. GeoMx™ RNA Assay: High
621 Multiplex, Digital, Spatial Analysis of RNA in FFPE Tissue. Methods in molecular biology.
622 2020;2148:331-45. Epub 2020/05/13. doi: 10.1007/978-1-0716-0623-0_21. PubMed PMID:
623 32394392.
624 25. Blumhagen RZ, Kurche JS, Cool CD, Walts AD, Heinz D, Fingerlin TE, et al. Spatially distinct
625 molecular patterns of gene expression in idiopathic pulmonary fibrosis. Respir Res.
626 2023;24(1):287. Epub 2023/11/18. doi: 10.1186/s12931-023-02572-6. PubMed PMID:
627 37978501; PubMed Central PMCID: PMCPMC10655274 outside the submitted work. Dr.
628 Schwartz is the founder and unpaid chief scientific officer of Eleven P15, Inc., and serves as
629 a consultant for Vertex Pharmaceuticals. Dr. Fingerlin and Dr. Yang report consulting fees from
630 Eleven P15, Inc., outside the submitted work and Drs. Schwartz, Fingerlin, and Yang have a
631 patent Methods and Compositions for Risk Prediction, Diagnosis, Prognosis, and Treatment
632 of Pulmonary Disorders issued. Dr. Cool reports consultant fees from Eleven P15, Inc. and
633 Theralink Technologies. Dr. Kurche, Avram Walts, and David Heinz report no competing
634 interests.
635 26. Pennel KAF, Hatthakarnkul P, Wood CS, Lian GY, Al-Badran SSF, Quinn JA, et al. JAK/STAT3
636 represents a therapeutic target for colorectal cancer patients with stromal-rich tumors. J Exp
637 Clin Cancer Res. 2024;43(1):64. Epub 2024/03/01. doi: 10.1186/s13046-024-02958-4.
638 PubMed PMID: 38424636; PubMed Central PMCID: PMCPMC10905886.
639 27. Liberzon A, Birger C, Thorvaldsdóttir H, Ghandi M, Mesirov JP, Tamayo P. The Molecular
640 Signatures Database (MSigDB) hallmark gene set collection. Cell Syst. 2015;1(6):417-25.
641 Epub 2016/01/16. doi: 10.1016/j.cels.2015.12.004. PubMed PMID: 26771021; PubMed
642 Central PMCID: PMCPMC4707969.

643 28. Subramanian A, Tamayo P, Mootha VK, Mukherjee S, Ebert BL, Gillette MA, et al. Gene set
644 enrichment analysis: a knowledge-based approach for interpreting genome-wide expression
645 profiles. Proc Natl Acad Sci U S A. 2005;102(43):15545-50. Epub 2005/10/04. doi:
646 10.1073/pnas.0506580102. PubMed PMID: 16199517; PubMed Central PMCID:
647 PMCPMC1239896.
648 29. Jin S, Guerrero-Juarez CF, Zhang L, Chang I, Ramos R, Kuan CH, et al. Inference and
649 analysis of cell-cell communication using CellChat. Nat Commun. 2021;12(1):1088. Epub
650 2021/02/19. doi: 10.1038/s41467-021-21246-9. PubMed PMID: 33597522; PubMed Central
651 PMCID: PMCPMC7889871.
652 30. Harada T, Iwabe T, Terakawa N. Role of cytokines in endometriosis. Fertility and Sterility.
653 2001;76(1):1-10. doi: https://doi.org/10.1016/S0015-0282(01)01816-7.
654 31. Noble LS, Simpson ER, Johns A, Bulun SE. Aromatase expression in endometriosis. J Clin
655 Endocrinol Metab. 1996;81(1):174-9. Epub 1996/01/01. doi: 10.1210/jcem.81.1.8550748.
656 PubMed PMID: 8550748.
657 32. Attia GR, Zeitoun K, Edwards D, Johns A, Carr BR, Bulun SE. Progesterone receptor isoform
658 A but not B is expressed in endometriosis. J Clin Endocrinol Metab. 2000;85(8):2897-902.
659 Epub 2000/08/18. doi: 10.1210/jcem.85.8.6739. PubMed PMID: 10946900.
660 33. Bulun SE, Yang S, Fang Z, Gurates B, Tamura M, Sebastian S. Estrogen production and
661 metabolism in endometriosis. Annals of the New York Academy of Sciences. 2002;955:75-85;
662 discussion 6-8, 396-406. Epub 2002/04/13. doi: 10.1111/j.1749-6632.2002.tb02767.x.
663 PubMed PMID: 11949967.
664 34. Fazleabas AT, Brudney A, Chai D, Langoi D, Bulun SE. Steroid receptor and aromatase
665 expression in baboon endometriotic lesions. Fertil Steril. 2003;80 Suppl 2:820-7. Epub
666 2003/09/25. doi: 10.1016/s0015-0282(03)00982-8. PubMed PMID: 14505759.
667 35. Attar E, Tokunaga H, Imir G, Yilmaz MB, Redwine D, Putman M, et al. Prostaglandin E2 via
668 steroidogenic factor-1 coordinately regulates transcription of steroidogenic genes necessary
669 for estrogen synthesis in endometriosis. J Clin Endocrinol Metab. 2009;94(2):623-31. Epub
670 2008/11/13. doi: 10.1210/jc.2008-1180. PubMed PMID: 19001523; PubMed Central PMCID:
671 PMCPMC2646521.
672 36. Yilmaz BD, Bulun SE. Endometriosis and nuclear receptors. Hum Reprod Update.
673 2019;25(4):473-85. doi: 10.1093/humupd/dmz005. PubMed Central PMCID:
674 PMCPMC6601390.
675 37. Ohlsson Teague EM, Van der Hoek KH, Van der Hoek MB, Perry N, Wagaarachchi P,
676 Robertson SA, et al. MicroRNA-regulated pathways associated with endometriosis. Mol

677 Endocrinol. 2009;23(2):265-75. Epub 2008/12/17. doi: 10.1210/me.2008-0387. PubMed
678 PMID: 19074548; PubMed Central PMCID: PMCPMC5419313.
679 38. Nothnick WB, Falcone T, Joshi N, Fazleabas AT, Graham A. Serum miR-451a Levels Are
680 Significantly Elevated in Women With Endometriosis and Recapitulated in Baboons (Papio
681 anubis) With Experimentally-Induced Disease. Reproductive sciences (Thousand Oaks,
682 Calif). 2017;24(8):1195-202. Epub 2016/12/07. doi: 10.1177/1933719116681519. PubMed
683 PMID: 27920341.
684 39. Rekker K, Tasa T, Saare M, Samuel K, Kadastik U, Karro H, et al. Differentially-Expressed
685 miRNAs in Ectopic Stromal Cells Contribute to Endometriosis Development: The Plausible
686 Role of miR-139-5p and miR-375. Int J Mol Sci. 2018;19(12). Epub 2018/11/30. doi:
687 10.3390/ijms19123789. PubMed PMID: 30487429; PubMed Central PMCID:
688 PMCPMC6321240.
689 40. Pavone ME, Grover AR, Confino R, Pearson EK, Malpani S, Cheng YH, et al. Retinoic acid
690 action is altered within endometrium of baboons affected with endometriosis. Journal of
691 Endometriosis and Pelvic Pain Disorders. 2022:22840265211062008. doi:
692 10.1177/22840265211062008. PubMed PMID: WOS:000740968400001.
693 41. Song Y, Su RW, Joshi NR, Kim TH, Lessey BA, Jeong JW, et al. Interleukin-6 (IL-6) Activates
694 the NOTCH1 Signaling Pathway Through E-Proteins in Endometriotic Lesions. J Clin
695 Endocrinol Metab. 2020;105(5). Epub 2020/03/03. doi: 10.1210/clinem/dgaa096. PubMed
696 PMID: 32119078; PubMed Central PMCID: PMCPMC7096313.
697 42. Kai K, Joshi NR, Burns GW, Hrbek SM, Vegter EL, Ochoa-Bernal MA, et al. MicroRNA-210-
698 3p Regulates Endometriotic Lesion Development by Targeting IGFBP3 in Baboons and
699 Women with Endometriosis. Reproductive sciences (Thousand Oaks, Calif).
700 2023;30(10):2932-44. Epub 2023/05/16. doi: 10.1007/s43032-023-01253-5. PubMed PMID:
701 37188982; PubMed Central PMCID: PMCPMC10556147.
702 43. Hogg C, Panir K, Dhami P, Rosser M, Mack M, Soong D, et al. Macrophages inhibit and
703 enhance endometriosis depending on their origin. Proc Natl Acad Sci U S A. 2021;118(6).
704 Epub 2021/02/05. doi: 10.1073/pnas.2013776118. PubMed PMID: 33536334.
705 44. Hogg C, Horne AW, Greaves E. Endometriosis-Associated Macrophages: Origin, Phenotype,
706 and Function. Front Endocrinol (Lausanne). 2020;11:7. Epub 2020/02/11. doi:
707 10.3389/fendo.2020.00007. PubMed PMID: 32038499; PubMed Central PMCID:
708 PMCPMC6989423.

45. Henlon Y, Panir K, McIntyre I, Hogg C, Dhami P, Cuff AO, et al. Single-cell analysis identifies distinct macrophage phenotypes associated with pro-disease and pro-resolving functions in the endometriotic niche. bioRxiv. 2024:2024.03.07.583861. doi: 10.1101/2024.03.07.583861.
46. Croasdell Lucchini A, Gachanja NN, Rossi AG, Dorward DA, Lucas CD. Epithelial Cells and Inflammation in Pulmonary Wound Repair. Cells. 2021;10(2). Epub 2021/02/11. doi: 10.3390/cells10020339. PubMed PMID: 33562816; PubMed Central PMCID: PMCPMC7914803.
47. Ren JL, Pan JS, Lu YP, Sun P, Han J. Inflammatory signaling and cellular senescence. Cell Signal. 2009;21(3):378-83. Epub 2008/11/11. doi: 10.1016/j.cellsig.2008.10.011. PubMed PMID: 18992324; PubMed Central PMCID: PMCPMC2870712.
48. Zou L, Meng L, Xu Y, Wang K, Zhang J. Revealing the diagnostic value and immune infiltration of senescence-related genes in endometriosis: a combined single-cell and machine learning analysis. Front Pharmacol. 2023;14:1259467. Epub 2023/10/20. doi: 10.3389/fphar.2023.1259467. PubMed PMID: 37860112; PubMed Central PMCID: PMCPMC10583561.
49. Muter J, Kong CS, Brosens JJ. The Role of Decidual Subpopulations in Implantation, Menstruation and Miscarriage. Front Reprod Health. 2021;3:804921. Epub 2022/10/29. doi: 10.3389/frph.2021.804921. PubMed PMID: 36303960; PubMed Central PMCID: PMCPMC9580781.
50. Crocker PR, Jefferies WA, Clark SJ, Chung LP, Gordon S. Species heterogeneity in macrophage expression of the CD4 antigen. J Exp Med. 1987;166(2):613-8. Epub 1987/08/01. doi: 10.1084/jem.166.2.613. PubMed PMID: 3110358; PubMed Central PMCID: PMCPMC2189597.
51. Zhen A, Krutzik SR, Levin BR, Kasparian S, Zack JA, Kitchen SG. CD4 ligation on human blood monocytes triggers macrophage differentiation and enhances HIV infection. J Virol. 2014;88(17):9934-46. Epub 2014/06/20. doi: 10.1128/jvi.00616-14. PubMed PMID: 24942581; PubMed Central PMCID: PMCPMC4136363.
52. Stevenson M. HIV-1 pathogenesis. Nat Med. 2003;9(7):853-60. Epub 2003/07/02. doi: 10.1038/nm0703-853. PubMed PMID: 12835705.
53. Betjes MG, Haks MC, Tuk CW, Beelen RH. Monoclonal antibody EBM11 (anti-CD68) discriminates between dendritic cells and macrophages after short-term culture. Immunobiology. 1991;183(1-2):79-87. Epub 1991/09/01. doi: 10.1016/s0171-2985(11)80187-7. PubMed PMID: 1834546.

742 54. Yan J, Zhou L, Liu M, Zhu H, Zhang X, Cai E, et al. Single-cell analysis reveals insights into
743 epithelial abnormalities in ovarian endometriosis. Cell Rep. 2024;43(3):113716. Epub
744 2024/02/27. doi: 10.1016/j.celrep.2024.113716. PubMed PMID: 38412094.
745 55. Calandra T, Roger T. Macrophage migration inhibitory factor: a regulator of innate immunity.
746 Nat Rev Immunol. 2003;3(10):791-800. Epub 2003/09/23. doi: 10.1038/nri1200. PubMed
747 PMID: 14502271; PubMed Central PMCID: PMCPMC7097468.
748 56. Mitchell RA, Metz CN, Peng T, Bucala R. Sustained mitogen-activated protein kinase (MAPK)
749 and cytoplasmic phospholipase A2 activation by macrophage migration inhibitory factor (MIF).
750 Regulatory role in cell proliferation and glucocorticoid action. J Biol Chem.
751 1999;274(25):18100-6. Epub 1999/06/11. doi: 10.1074/jbc.274.25.18100. PubMed PMID:
752 10364264.
753 57. Schenkein HA, Rutherford B. C3-mediated release of prostaglandin from human monocytes.
754 Behaviour in short-term culture. Immunology. 1984;51(1):83-91. Epub 1984/01/01. PubMed
755 PMID: 6690398; PubMed Central PMCID: PMCPMC1454415.
756 58. Calandra T, Bernhagen J, Mitchell RA, Bucala R. The macrophage is an important and
757 previously unrecognized source of macrophage migration inhibitory factor. J Exp Med.
758 1994;179(6):1895-902. Epub 1994/06/01. doi: 10.1084/jem.179.6.1895. PubMed PMID:
759 8195715; PubMed Central PMCID: PMCPMC2191507.
760 59. Bacher M, Metz CN, Calandra T, Mayer K, Chesney J, Lohoff M, et al. An essential regulatory
761 role for macrophage migration inhibitory factor in T-cell activation. Proc Natl Acad Sci U S A.
762 1996;93(15):7849-54. Epub 1996/07/23. doi: 10.1073/pnas.93.15.7849. PubMed PMID:
763 8755565; PubMed Central PMCID: PMCPMC38837.
764 60. Weed JC, Arquembourg PC. Endometriosis: can it produce an autoimmune response
765 resulting in infertility? Clin Obstet Gynecol. 1980;23(3):885-93. Epub 1980/09/01. PubMed
766 PMID: 7418287.
767 61. Isaacson KB, Coutifaris C, Garcia CR, Lyttle CR. Production and secretion of complement
768 component 3 by endometriotic tissue. J Clin Endocrinol Metab. 1989;69(5):1003-9. Epub
769 1989/11/01. doi: 10.1210/jcem-69-5-1003. PubMed PMID: 2793987.
770 62. Tao XJ, Sayegh RA, Isaacson KB. Increased expression of complement component 3 in
771 human ectopic endometrium compared with the matched eutopic endometrium. Fertil Steril.
772 1997;68(3):460-7. Epub 1997/10/07. doi: 10.1016/s0015-0282(97)00254-9. PubMed PMID:
773 9314915.

774 63. Hasan A, Rahim A, Afzal M, Naveed AK, Ayub S, Jahan S. Serum Albumin and C3
775 Complement Levels in Endometriosis. J Coll Physicians Surg Pak. 2019;29(8):702-5. Epub
776 2019/07/31. doi: 10.29271/jcpsp.2019.08.702. PubMed PMID: 31358086.
777 64. Young SL. The complement system and its role in the endometrium. In: Aplin JD, Fazleabas
778 AT, Glasser SR, Giudice LC, editors. The Endometrium: Molecular, Cellular and Clinical
779 Perspectives, Second Edition: Taylor & Francis; 2008. p. 568-78.
780 65. Agostinis C, Balduit A, Mangogna A, Zito G, Romano F, Ricci G, et al. Immunological Basis of
781 the Endometriosis: The Complement System as a Potential Therapeutic Target. Front
782 Immunol. 2020;11:599117. Epub 2021/01/29. doi: 10.3389/fimmu.2020.599117. PubMed
783 PMID: 33505394; PubMed Central PMCID: PMCPMC7829336.
784 66. Brown EJ, Frazier WA. Integrin-associated protein (CD47) and its ligands. Trends Cell Biol.
785 2001;11(3):130-5. Epub 2001/04/18. doi: 10.1016/s0962-8924(00)01906-1. PubMed PMID:
786 11306274.
787 67. Gresham HD, Dale BM, Potter JW, Chang PW, Vines CM, Lowell CA, et al. Negative
788 regulation of phagocytosis in murine macrophages by the Src kinase family member, Fgr. J
789 Exp Med. 2000;191(3):515-28. Epub 2000/02/09. doi: 10.1084/jem.191.3.515. PubMed
790 PMID: 10662797; PubMed Central PMCID: PMCPMC2195814.
791 68. Meri S, Morgan BP, Davies A, Daniels RH, Olavesen MG, Waldmann H, et al. Human protectin
792 (CD59), an 18,000-20,000 MW complement lysis restricting factor, inhibits C5b-8 catalysed
793 insertion of C9 into lipid bilayers. Immunology. 1990;71(1):1-9. Epub 1990/09/01. PubMed
794 PMID: 1698710; PubMed Central PMCID: PMCPMC1384213.
795 69. Yang H, Li L, Liu X, Zhao Y. High Expression of the Component 3a Receptor 1 (C3AR1) Gene
796 in Stomach Adenocarcinomas Infers a Poor Prognosis and High Immune-Infiltration Levels.
797 Med Sci Monit. 2021;27:e927977. Epub 2021/02/05. doi: 10.12659/msm.927977. PubMed
798 PMID: 33539329; PubMed Central PMCID: PMCPMC7871482.
799 70. Zhu S, Wang A, Xu W, Hu L, Sun J, Wang X. The heterogeneity of fibrosis and angiogenesis
800 in endometriosis revealed by single-cell RNA-sequencing. Biochim Biophys Acta Mol Basis
801 Dis. 2023;1869(2):166602. Epub 2022/11/19. doi: 10.1016/j.bbadis.2022.166602. PubMed
802 PMID: 36400338.
803 71. Sunderkötter C, Steinbrink K, Goebeler M, Bhardwaj R, Sorg C. Macrophages and
804 angiogenesis. J Leukoc Biol. 1994;55(3):410-22. Epub 1994/03/01. doi: 10.1002/jlb.55.3.410.
805 PubMed PMID: 7509844.
806 72. Martínez-Ramos S, Rafael-Vidal C, Malvar-Fernández B, Pérez N, Mouriño C, Pérez SG, et
807 al. Semaphorin3B promotes an anti-inflammatory and pro-resolving phenotype in

macrophages from rheumatoid arthritis patients in a MerTK-dependent manner. Front Immunol. 2023;14:1268144. Epub 2024/01/29. doi: 10.3389/fimmu.2023.1268144. PubMed PMID: 38283352; PubMed Central PMCID: PMCPMC10811190.

73. Bulun SE, Fang Z, Imir G, Gurates B, Tamura M, Yilmaz B, et al. Aromatase and endometriosis. Semin Reprod Med. 2004;22(1):45-50. Epub 2004/04/15. doi: 10.1055/s-2004-823026. PubMed PMID: 15083380.
74. Ullah K, Rahman TU, Pan HT, Guo MX, Dong XY, Liu J, et al. Serum estradiol levels in controlled ovarian stimulation directly affect the endometrium. J Mol Endocrinol. 2017;59(2):105-19. Epub 2017/05/26. doi: 10.1530/jme-17-0036. PubMed PMID: 28539318; PubMed Central PMCID: PMCPMC5510595.
75. Agostinis C, Zorzet S, Balduit A, Zito G, Mangogna A, Macor P, et al. The Inflammatory Feed-Forward Loop Triggered by the Complement Component C3 as a Potential Target in Endometriosis. Front Immunol. 2021;12:693118. Epub 2021/09/08. doi: 10.3389/fimmu.2021.693118. PubMed PMID: 34489939; PubMed Central PMCID: PMCPMC8418148.
76. Ruiz LA, Baez-Vega PM, Ruiz A, Peterse DP, Monteiro JB, Bracero N, et al. Dysregulation of Lysyl Oxidase Expression in Lesions and Endometrium of Women With Endometriosis. Reproductive sciences (Thousand Oaks, Calif). 2015;22(12):1496-508. Epub 2015/05/13. doi: 10.1177/1933719115585144. PubMed PMID: 25963914; PubMed Central PMCID: PMCPMC5933196.
77. Colon-Diaz M, Baez-Vega P, Garcia M, Ruiz A, Monteiro JB, Fourquet J, et al. HDAC1 and HDAC2 are differentially expressed in endometriosis. Reproductive sciences (Thousand Oaks, Calif). 2012;19(5):483-92. Epub 2012/02/22. doi: 10.1177/1933719111432870. PubMed PMID: 22344732; PubMed Central PMCID: PMCPMC3343094 research, authorship, and/or publication of this article.
78. Colón-Caraballo M, García M, Mendoza A, Flores I. Human Endometriosis Tissue Microarray Reveals Site-specific Expression of Estrogen Receptors, Progesterone Receptor, and Ki67. Appl Immunohistochem Mol Morphol. 2019;27(7):491-500. Epub 2018/04/10. doi: 10.1097/pai.0000000000000663. PubMed PMID: 29629944; PubMed Central PMCID: PMCPMC6174114.
79. Noyes RW, Hertig AT, Rock J. Dating the endometrial biopsy. American journal of obstetrics and gynecology. 1975;122(2):262-3. Epub 1975/05/01. doi: 10.1016/s0002-9378(16)33500-1. PubMed PMID: 1155504.

80. McInnes L, Healy J, Melville J. Umap: Uniform manifold approximation and projection for dimension reduction. arXiv preprint arXiv:180203426. 2018.
81. Team R. RStudio: Integrated Development for R. Boston, MA: RStudio, PBC.; 2020. Available from: http://www.rstudio.com/.
82. Zhou X, Lindsay H, Robinson MD. Robustly detecting differential expression in RNA sequencing data using observation weights. Nucleic Acids Res. 2014;42(11):e91. Epub 2014/04/23. doi: 10.1093/nar/gku310. PubMed PMID: 24753412; PubMed Central PMCID: PMCPMC4066750.